

# Temperature Feedback Based Heating Strategy for Ultrasound Thermal Surgery

Kuen-Cheng Ju, Shen-Li Fu

**Abstract**— Phased array transducer has the ability to generate multiple-focus pattern by adjusting the driving signal of individual element of the array. For the treatment of large target volume, several multiple-focus pattern could be used by using temporal switching technique among these power patterns. Typically, to obtain a uniform thermal dose, properly adjust the power level within the target volume is important. In this study, we proposed a temperature feedback based heating strategy without the need of power level adjustment. Several parameters, such as the setting temperature, sonication time, power level and blood perfusion, may affect the final thermal dose. Simulation results show that setting temperature is the key parameter to determine the final thermal dose while the effects of blood perfusion could be neglected and the sonication time should be as short as possible. Small power level is not suggested because the resulting thermal dose would extended owing to the thermal conduction.

## I. INTRODUCTION

HIGH intensity focused ultrasound (HIFU) is a new modality for ablating solid tumors, such as uterine fibroids and benign prostate hyperplasia and cancers of liver, kidney, prostate and breast [1-6]. The nature of focused ultrasound is that the ultrasound energy can be focused to induce a localized high temperature region and result in irreversible tissue necrosis. The focus of a single focused HIFU transducer is small and the resulting thermal lesion is also small. When the target volume is large, several lesions to cover the target volume is needed. To prevent the prefocal heating, cooling time between lesions is required which consequently result in the increase of total treatment time. Phased array transducer is capable of generating multiple-focus power pattern by adjusting the phase and amplitude of the driving signal of each individual element of the array; hence, a larger thermal lesion could be obtained. Wan [7] compares the difference between single and multiple focus power pattern on thermal dose distribution and treatment time. Their results indicate that by properly adjusting the power levels of the multiple-focus patterns could result in a uniform dose distribution and significantly reduce the treatment time. However, they did not state how the power levels were adjusted. Daum [8] proposed a temporal switching technique for HIFU heating which several power patterns

were sequentially sonicated to obtain a uniform thermal dose distribution. The power levels of the focus patterns were obtained via a previous optimization procedure. Lin [9] proposed a theoretical model to investigate the optimization of power deposition. An ideally “uniform” power and temperature pattern were assumed on a  $10 \times 10 \text{ mm}^2$  control plane. However, in practical, it is difficult to produce an uniform power or temperature pattern.

In this study, we proposed a heating strategy based on temperature feedback. Several multiple-focused power patterns with the same power level were temporally and repeatedly sonicated until the foci reached a predetermined setting temperature. Besides the setting temperature, the sonication time of each power pattern, blood perfusion and power level are the parameters may affect the thermal dose distribution. We examine the relationship between those parameters and the resulting temperature and thermal dose responses. The proposed heating strategy could be an alternative method for thermal lesion control during HIFU thermal therapy.

## II. METHODS

### A. HIFU System and heating strategy

A spherical phased-array transducer with a radius of 120 mm and a diameter of 100 mm was assumed in this study. Foci were arranged on a  $10 \times 10 \text{ mm}^2$  (X-Y plane) control plane located at a depth of 120 mm (Z-Axis) from the center of the transducer. Six power patterns which consist of single or multiple foci were used to cover the target on the control plane (Fig. 1). Several temperature sensor points were arranged at each focus of all power patterns. The intensities of all the power patterns were assumed to be the same. During heating, the sonications rapidly changed between these six power patterns with a sonication time,  $t_s$ . Initially, all of the power patterns were used to raise the temperature. Temperature data are collected at the end of each sonication. Once the temperature of the sensor point is higher than the setting temperature,  $T_{set}$ , the corresponding power pattern was neglected during the following heating cycles. The heating was stopped when all the sensor points had been heated to  $T_{set}$ .

### B. Acoustical Model

The acoustic model was a simple water-tissue model, assuming the density and the speed of sound in the two layers are close, the reflection and refraction at the water-tissue interface can be ignored [9]. The acoustic pressure field generated by the ultrasound transducer was calculated

This work was supported in part by National Science Council of Taiwan with Grant No. NSC 100-2221-E-214 -022 and NSC 99-2632-E-214-001-MY3-3.

K. C. Ju is with the Department of Biomedical Engineering, I-Shou University, Kaohsiung, 82445 Taiwan (e-mail: [kcju@isu.edu.tw](mailto:kcju@isu.edu.tw)).

S. L. Fu is with the Department of Electrical Engineering, I-Shou University, Kaohsiung, 82445 Taiwan

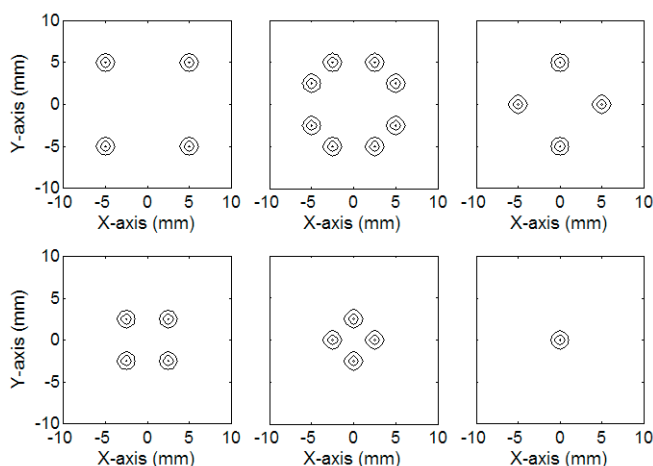


Figure 1. Power patterns used in this study.

by using the Rayleigh–Sommerfeld integral to sum up the contribution of each point source on the surface of the transducer.

$$p(x, y, z) = \frac{i\rho ck}{2\pi} \int u \frac{e^{-(\alpha+ik)(r-r')}}{|r-r'|} dS \quad (1)$$

The multiple-focus pattern was approximated by the superposition of single-focus patterns [7]. Parameters used in this simulation are listed in Table I. The absorbed power density can be obtained from

$$q = \frac{\alpha|p|^2}{\rho c} \quad (2)$$

where  $\alpha$  is the ultrasound absorption coefficient of tissue,  $\rho$  is the tissue density,  $c$  is the speed of sound. In this study, the absorption coefficient was set to be the same as the attenuation coefficient of the ultrasound within tissues, assuming that the attenuated power is absorbed locally.

### C. Thermal Model

The temperature response produced by focused field can be calculated by the bioheat transfer equation (BHTE) [10]

$$\rho c_t \frac{\partial T}{\partial t} = k \nabla^2 T - w_b c_b (T - T_{ar}) + q \quad (3)$$

The absorbed acoustic power deposition  $q$  obtained from (2) was substituted into the BHTE and a three-dimensional finite

TABLE I  
PARAMETERS USED IN ACOUSTIC AND THERMAL MODEL

Symbol	Parameters	Value
$c$	speed of sound	1500 m/s
$\rho$	tissue density	1000 kg/m <sup>3</sup>
$\alpha$	absorption coefficient	5 Np/m
$K$	thermal conductivity	0.5 W/m°C
$c_t/c_b$	specific heat(tissue / blood)	3770 J/kg°C
$w_b$	blood perfusion rate	5 kg/m <sup>3</sup> s

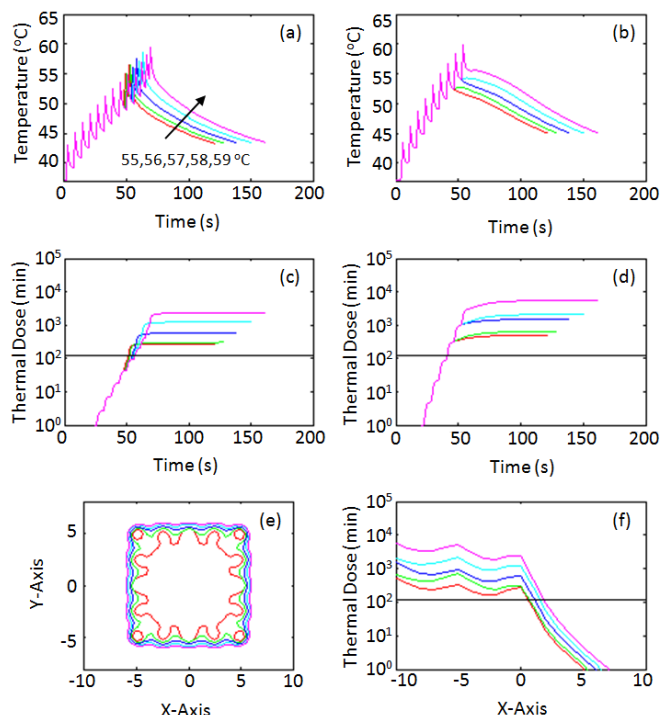


Figure 2. Results for setting temperature varies from 55°C to 59°C. (a) and (b) are temperature responses at the boundary and center of the target, respectively. (c) and (d) are thermal dose responses corresponding to (a) and (b). (e) and (f) are the contour for thermal dose larger than 120 min and the distribution of thermal dose along X-Axis.

difference method was used to determine the temperature response.

A thermal dose (TD) is used to quantify the effect of temperature and heating duration on tissues and to estimate the necrotic tissue volume, and it was numerically modeled using the following equation [11-12]:

$$TD = \int_{t_0}^{t_f} R^{(T-43)} dt \quad (4)$$

where  $R = 2$  for  $T \geq 43^\circ\text{C}$  and  $R = 4$  for  $37^\circ\text{C} < T < 43^\circ\text{C}$ .  $t_0$  is the start time of heating and  $t_f$  is the time when temperature is  $37^\circ\text{C}$ . The range of the thermal dose causing necrosis for soft tissue is from 50 to 240 min [13-14]. In this study, an average value of 120 min thermal dose was considered to be the threshold value for successful treatment.

### III. RESULTS AND DISCUSSION

The setting temperature,  $T_{\text{set}}$ , is a parameter potentially affecting the temperature response and the accumulated thermal dose. Fig. 2 shows the simulation results for  $T_{\text{set}}$  varied from 55°C to 59°C when the sonication time is 1.0 sec, blood perfusion is 5 kg/m<sup>3</sup>s and the intensity of foci is 300W/cm<sup>2</sup>. Fig. 2(a) and 2(b) are the temperature responses at the boundary and the center of the target at the control plane, respectively. During the heating, the temperature elevation is vibrated owing to the temporal-switched sonication heating strategy. Although, the temperature is vibrated, it almost linearly increases with time. In addition, the heating rate is higher at the central portion than that at the boundary. During

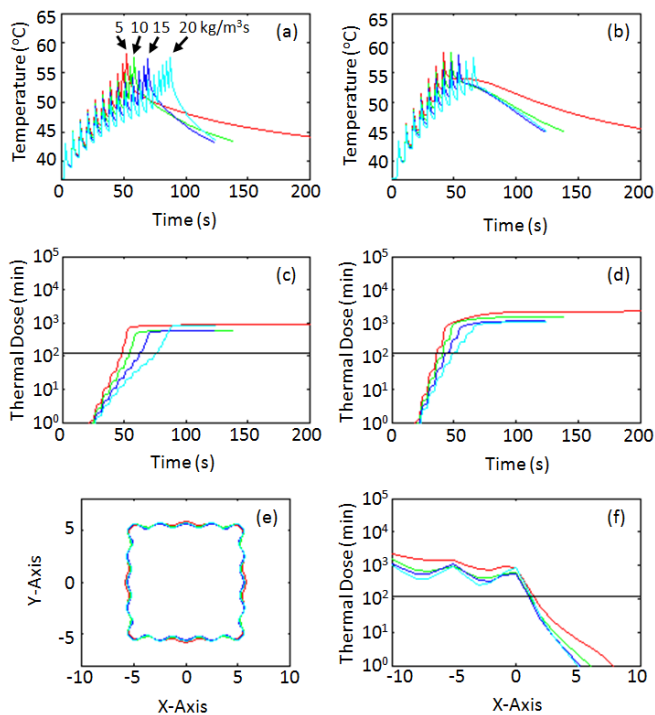


Figure 3. Results for blood perfusion varies from  $5 \text{ kg/m}^3\text{s}$  to  $20 \text{ kg/m}^3\text{s}$ . (a) and (b) are temperature responses at the boundary and center of the target, respectively. (c) and (d) are thermal dose responses corresponding to (a) and (b). (e) and (f) are the contour for thermal dose larger than 120 min and the distribution of thermal dose along X-Axis.

the cooling, the temperature curves are almost parallelly decreased with time and the cooling rate at the boundary is higher than that at the central portion. Fig. 2(c) and 2(d) are the accumulated thermal dose corresponding to the temperatures in Fig. 2(a) and 2(b), respectively. Obviously, thermal doses are accumulated to the therapeutic level ( $> 120$  min) during the heating phase and the final thermal doses are larger than the required doses. Fig. 2(e) and 2(f) show the region with thermal dose larger than 120 min ( $TD_{120}$ ) on the control plane and the distribution of thermal dose along X-Axis, respectively, for different setting temperature. It can be seen that, a higher setting temperature can result in a larger  $TD_{120}$  region, which even covers the boundary and the corner of the target. On the other hand, for a lower setting temperature, the resulting thermal doses at the intervening region among foci may lower than required, especially at the region near the boundary and the corner of the target, where the heat conduction are strong.

To investigate the effect of blood perfusion on the temperature response and thermal dose, the blood perfusion is varied from  $5 \text{ kg/m}^3\text{s}$  to  $20 \text{ kg/m}^3\text{s}$  and the setting temperature is stay at  $57^\circ\text{C}$  while the other parameters are the same as the simulation in Fig. 2. Fig. 3 shows the simulation results. Obviously, blood perfusion affects the temperature elevation. It takes more time to reach the setting temperature when perfusion is large while the temperature is sharply decreased during the cooling phase. At the boundary, thermal dose accumulation is quickly stopped when ultrasound is turned off because of the sharply decreased temperature (Fig. 3(c)). It could be resulted from the strong thermal conduction at the

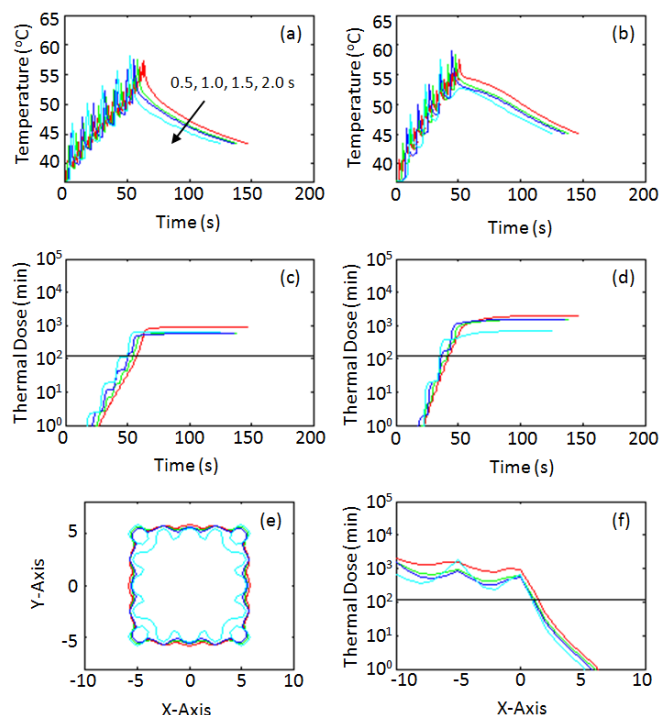


Figure 4. Results for sonication time varies from 0.5 s to 2.0 s. (a) and (b) are temperature responses at the boundary and center of the target, respectively. (c) and (d) are thermal dose responses corresponding to (a) and (b). (e) and (f) are the contour for thermal dose larger than 120 min and the distribution of thermal dose along X-Axis.

boundary. On the other hand, the slopes of the turning point of the thermal dose curves in Fig. 3(d) are related to the values of blood perfusion. For small perfusion rate, thermal dose still gently increased even though the ultrasound has been turned off. Although the final thermal doses varies with different blood perfusion levels within the target, they almost converge together on the boundary owing to the strong thermal conduction. Hence, the final shape of  $TD_{120}$  (Fig. 3(e)) seems to be independent of blood perfusion.

The above results show that setting temperature is a key parameter that affects the shape of  $TD_{120}$  and it is almost independent of blood perfusion. However, some technical parameter should be considered, such as the sonication time and power level of each ultrasound power pattern. In this simulation, the sonication times varies from 0.5 s to 2 s and the setting temperature stay at  $57^\circ\text{C}$  while the other parameters are the same as the simulation in Fig. 2. Fig. 4(a) and 4(b) are the temperature response at the boundary and the center of the target at the control plane, respectively. During heating, the temperature is raised to the target temperature with fluctuations and it's amplitude is proportional to the sonication time. For longer sonication time, it requires less heating cycles to reach the target temperature with larger temperature fluctuation. These large fluctuations can also be observed on the thermal dose accumulation (Fig. 4(c) and 4(d)). The stepped increased thermal doses for longer sonication time are resulted from the larger temperature fluctuations. Fig. 4(e) shows the  $TD_{120}$  region on the control plane. The intervening portion among foci is heated by the thermal conduction from foci; however, when the sonication time is too long, the

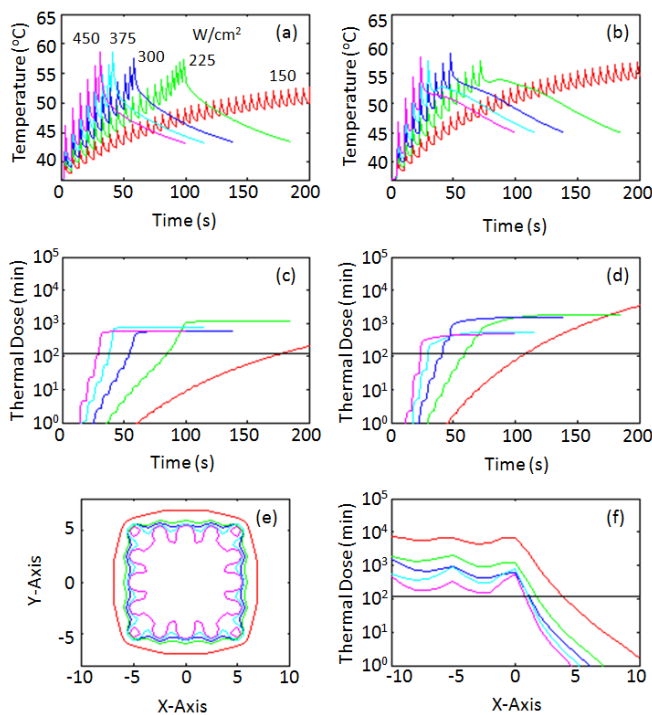


Figure 5. Results for power level varies from 150 W to 450 W. (a) and (b) are temperature responses at the boundary and center of the target, respectively. (c) and (d) are thermal dose responses corresponding to (a) and (b). (e) and (f) are the contour for thermal dose larger than 120 min and the distribution of thermal dose along X-Axis.

temperature at foci sharply increased and decreased, resulting in the intervening portion among foci may not accumulate sufficient thermal dose. This effect can be observed in the valleys of the curves of Fig. 4(f). Hence, it is suggested that the sonication time should be as short as possible.

Similar to the sonication time, a larger ultrasound power could result in sharp temperature increase and decrease. Fig. 5 simulate the effects of the ultrasound intensity on the temperature and thermal dose responses. The intensity of foci varies from 150 W/cm<sup>2</sup> to 450 W/cm<sup>2</sup> and the setting temperature keep at 57°C while the other parameters are the same as the simulation in Fig. 2. It can be seen that the temperatures are increased to the setting temperature with fluctuations, which the amplitudes is related to the intensities of foci. At expected, the time needed to reach the target temperature is inverse proportional to ultrasound intensities. For small ultrasound intensity level, the heating rate is slow; however, the final thermal dose is larger than high intensity cases while the TD<sub>120</sub> region is extended due to the thermal conduction on the boundary (Fig. 5(e)). Similar to the long sonication time case (Fig. 4(f)), the temperature sharply increase and decrease which result in the valleys of the curve in Fig. 5(f) when large ultrasound intensities are used. Hence, too small or too large ultrasound intensity should be avoided for the proposed heating strategy.

#### IV. CONCLUSION

Temporal switching of several multiple-focus power patterns has been shown to be capable of generate uniform thermal dose for large treatment volume. The essential of successful treatment is appropriate ultrasound power deposition. In this study, we proposed a temperature feedback heating strategy instead of an off-line power optimization procedure. By properly select the heating parameters, uniform thermal dose could be obtained without power level adjustment.

#### REFERENCES

- [1] C. M. C. Tempny, E. A. Stewart and N. McDannold et al., "MR imaging-guided focused ultrasound surgery of uterine leiomyomas: a feasibility study," *Radiology*, vol. 226, pp. 897–905, 2003
- [2] N. T. Sanghvi, R. S. Foster and B. Bihle R et al., "Noninvasive surgery of prostate tissue by high intensity focused ultrasound: an updated report," *Eur.J. Ultrasound*, vol. 9, pp. 19–29, 1999
- [3] F. Wu, Z.B. Wang and W. Z. Chen et al., "Extracorporeal high intensity focused ultrasound ablation in the treatment of patients with large hepatocellular carcinoma," *Ann.Surg. Oncol.*, vol. 11, pp. 1061–1069, 2004
- [4] K. U. Kohrmann, M.S. Michel and J. Gaa et al., "High intensity focused ultrasound as noninvasive therapy for multilocal renal cell carcinoma: case study and review of the literature," *J. Urol.*, vol. 167, pp. 2397–2403, 2002
- [5] G. Vallancien, D. Prapotnich and X. Cathelineau et al., "Transrectal focused ultrasound combined with transurethral resection of the prostate for the treatment of localized prostate cancer: feasibility study," *J. Urol.*, vol. 171, pp. 2265–2270, 2004
- [6] K. Hynynen K, O. Pomeroy and D. N. Smith et al., "MR imaging-guided focused ultrasound surgery of fibroadenomas in the breast: a feasibility study," *Radiology*, Vol. 219, pp. 176–185, 2001
- [7] H. Wan, P. VanBaren and E.S. Ebbini, "Ultrasound surgery: comparison of strategies using phased array systems," *IEEE Trans.Ultrasound, Ferroelect., Freq. Contr.*, vol. 43, pp. 1085–1097, 1996
- [8] D.R. Daum and K. Hynynen, "Thermal dose optimization via temporal switching in ultrasound surgery," *IEEE Trans.Ultrasound, Ferroelect., Freq. Contr.*, vol. 45, pp. 208–215, 1998
- [9] W.L. Lin, T.C. Liang and J.Y. Yen et al., "Optimization of power deposition and a heating strategy for external ultrasound thermal therapy," *Med. Phys.*, vol. 28, pp. 2172–2181, 2001
- [10] H. H. Pennes, "Analysis of tissue and arterial blood temperatures in the resting human forearm," *J. Appl. Physiol.*, vol. 1, pp. 19–122, 1948
- [11] W. C. Dewey, "Arrhenius relationships from the molecule and cell to the clinic," *Int. J. Hypertherm.*, vol. 10, pp. 457–483, 1994
- [12] S. A. Sapareto and W. C. Dewey, "Thermal dose determination in cancer therapy," *Int. J. Radiat. Oncol. Biol. Phys.*, vol. 10, pp. 787–800, 1984